

## Supplementary Information

### AGuIX nanoparticle-nanobody bioconjugates to target immune checkpoint receptors

Léna Carmès<sup>a,b\*</sup>, Guillaume Bort<sup>a\*</sup>, François Lux<sup>a,c†</sup>, Léa Seban<sup>d</sup>, Paul Rocchi<sup>a,b</sup>, Zeinaf Muradova<sup>d</sup>, Agnes Hagège<sup>e</sup>, Laurence Heinrich-Balard<sup>f</sup>, Frédéric Delolme<sup>g</sup>, Virginie Gueguen-chaignon<sup>g</sup>, Charles Truillet<sup>h</sup>, Stephanie Crowley<sup>i</sup>, Elisa Bello<sup>i</sup>, Tristan Doussineau<sup>b</sup>, Michael Dougan<sup>ij</sup>, Olivier Tillement<sup>a</sup>, Jonathan D. Schoenfeld<sup>d</sup>, Needa Brown<sup>d,k†</sup> and Ross Berbeco<sup>d†</sup>

#### 1. Chemical products

Phosphate-Buffered Saline (PBS), dimethyl sulfoxide (DMSO, >99.5%), ammonium acetate (CH<sub>3</sub>CO<sub>2</sub>NH<sub>4</sub>, >99.9%), and acetic acid glacial (C<sub>2</sub>H<sub>4</sub>O<sub>2</sub>, > 99.9%) were purchased from Sigma Aldrich (Germany). The gadolinium-chelated polysiloxane nanoparticles (AGuIX) were provided by NH TherAguix (Grenoble, France) as a lyophilized powder. The VHH A12 A4 and a heptamutant variant of *S. aureus* Sortase (StrA7m) were provided by the Massachusetts General Hospital (USA).<sup>1</sup> DBCO-PEG<sub>5</sub>-NHS ester and Azido-PEG<sub>4</sub>-NHS ester were purchased from BroadPharm (San Diego, CA). The fluorescent dyes, Lumiprobe Cy5.5-NHS ester (Cy5.5-NHS) and Alexa Fluor™ 647 Azide (AF647-azide) and the reactif N-(γ-maleimidobutyryloxy) succinimide ester (GMBS) were purchased from Thermo Fischer Scientific. Only milli-Q water (ρ > 18 MΩ.cm) was used to prepare aqueous solutions of nanoparticles (NPs). Each AGuIX NPs concentration is stated in g.L<sup>-1</sup> of gadolinium element.

Sequence of A12<sup>2</sup>:

QVQLVESGGGLVQAGGSLRLSCTASGSTFSRNAMAWFRQAPGKEREFVSGISRTGTNSYDADSVKGRFTISKDNAKNTVTLQMNSLKPEDTAIY  
YCALSQTASVATTERLYPYWGQGTQVTVSSGGLPETGGHHHHHH

Sequence of A4<sup>3</sup>:

MKYLPTAAAGLLLLAAQPAMAQVQLVESGGGLVPEGGSLRLSCAASGIIKINDMGWYRQAPGRREWVAASTGGDEAIYRDSVKDRFTISRDA  
KNSVFLQMNSLKPEDTAVYYCTAVISTDRDGTWRRYWGQGTQVTVSSGGLPETGGHHHHHH

#### 2. Synthesis of AGuIX@VHH through sortagging

##### 2.1. Synthesis of AGuIX@Mal

AGuIX NP (10 g, 13.28 w% Gd, ~15 Gd/NP) were dispersed in MilliQ water (200 g.L<sup>-1</sup>) and stirred for 30 min. Then, a solution of N-(γ-maleimidobutyryloxy) succinimide ester (GMBS, 50.0 mg, 178 μmol) in DMSO (420 μL) was added and the mixture was stirred for another 1 h. The AGuIX-Mal NP was purified by filtration (5 kDa MWCO turbo vivaspin, dilution x81) until no more maleimide (Mal) moiety could be detected in the filtrate and was finally dispersed into 4.4 mL of MilliQ water before lyophilisation. Mal quantification was performed by incubation with L-cystein (20 min, room temperature (RT)) and determination of the unreacted L-cystein with the photometric Ellman's test (Thermo Scientific, absorbance: 412 nm). The number of Mal moieties introduced on the surface of AGuIX NP could be modified in the range 0.3-2 Mal/NP by adjusting the amount of GMBS added.

##### 2.2. Synthesis of AGuIX@C(W/T) GGG

AGuIX-Mal (1.3 g, 15.0 w% Gd, 17.98 nmol Mal/mg AGuIX-Mal, 0.283 Mal/NP (~15 Gd/NP), 100 mg AGuIX-Mal/mL final concentration in reaction, redispersed in MilliQ H<sub>2</sub>O) and GGG(W/T)C (26 μmol, 20 nmol GGG(W/T)C/mg AGuIX-Mal, 2.0 mM final concentration in reaction, dispersed in PBS) were introduced in PBS (final volume 13 mL). The mixture was stirred (orbital) at RT for 6 h. The final product AGuIX-C(W/T) GGG was finally filtered (5 kDa MWCO turbo vivaspin, dilution x320) and stored at -20 °C (18,1 mL, 2.79 mg Gd/mL, 17.8 mM Gd). Quantification of the coupling reaction yield was determined for the synthesis of AGuIX-CWGGG using SEC method A, taking advantage of the fluorescence of tryptophan residues.

##### 2.3. Synthesis of AGuIX@Cy5.5-CTGGG

###### Step 1 – Introduction of Cy5.5

AGuIX-Mal NP (600 mg, 13.51 w% Gd, 50 mg AGuIX-Mal/mL final concentration in reaction, redispersed in MilliQ H<sub>2</sub>O) and Cy5.5-NHS ester (1.03 μmol, 85.9 μM final concentration in reaction) were introduced in H<sub>2</sub>O (final volume 12 mL). The mixture was stirred at RT for 30 min. After x2 dilution in H<sub>2</sub>O, the AGuIX-Cy5.5 was purified by filtration (5 kDa MWCO vivaspin, dilution x2).

###### Step 2 – Introduction of GGGTC

AGuIX-Cy5.5 (600 mg, 13.51 w% Gd, 123 nmolMal/mgAGuIX, 2.1 Mal/NP (~15 Gd/NP), 46 mg AGuIX-Cy5.5/mL final concentration in reaction, redispersed in MilliQ H<sub>2</sub>O) and GGGTC (78 μmol, 130 nmol GGGTC/mg AGuIX-Cy5.5, 6.0 mM final

concentration in reaction, dispersed in PBS) were introduced in PBS (final volume 13.0 mL). The mixture was stirred (orbital) at RT for 4.5 h and left overnight at 4 °C. The final product AGuIX-Cy5.5-CTGGG was finally filtered (5 kDa MWCO vivaspin, dilution x3125) and stored at -20 °C.

#### 2.4. Optimisation of sortagging reaction

AGuIX NPs were modified to mimic the functionality of the N-terminal oligoglycine residue typically employed in sortagging. Initially, a Mal functional group was introduced onto the surface of AGuIX NP through the use of a bifunctional NHS/Mal linker. This linker takes advantage of the amino groups present on AGuIX NP. By adjusting the ratio of linker to AGuIX NP, the number of grafted Mal groups could be controlled. This allowed for the production of AGuIX NPs carrying from 0.3 to 2 Mal groups per AGuIX NP (considering 15 Gd/NP). The low Mal/NP ratio could be beneficial if low amount of blocking agent is required compared to AGuIX NP (for therapeutic purpose). However, for effective MRI monitoring, it is crucial to ensure that a significant portion of AGuIX NPs is modified with VHH to minimize background signal originating from nonspecific AGuIX NPs. Consequently, AGuIX-Mal was further modified with a short peptide linker that incorporates a cysteine amino acid at the C-terminal and a triglycine residue (GGG) at the N-terminal. This modification allows for reactions to occur on both AGuIX-Mal and during sortagging, respectively. An additional tryptophan residue was introduced to create the peptide GGGWC, facilitating reaction monitoring using fluorescence detection. AGuIX-CWGGG was obtained following the coupling of the C-terminated peptide to AGuIX-Mal and subsequently purified through filtration to remove any residual unreacted linkers.

To enable the use of sortagging, the VHH was engineered by incorporating a C-terminal StrA motif LPETGG and a 6xHis tag. The addition of the 6xHis tag motif facilitated protein purification and removal of the C-terminal residue released during sortagging.<sup>1</sup> In this study, the mutant StrA7m was employed as it displayed improved kinetics and allowed for calcium-independent ligation.<sup>4</sup> The transpeptidation reaction between A12 and AGuIX-CWGGG was confirmed using SEC monitoring, and the presence of StrA7m was demonstrated to be necessary for the reaction to occur (Figure S1a-d). The equilibrium for the reaction was reached within 2-3 h at RT. Following isolation using Ni-beads to capture and remove the 6xHis-containing reagents and by-products (StrA7m, residual peptides from VHH C-terminal, and unreacted VHH), AGuIX@A12 was purified via filtration and dispersed in PBS.

To accurately determine the sortagging yield, the non-fluorescent starting material AGuIX-CTGGG was used to avoid interference with VHH fluorescence. A conversion rate of 43% for VHH was achieved during the sortagging process, resulting in an isolated yield of AGuIX@A12 of 5.3% (relative to A12) with a NP/A12 ratio of 20 (Figures S1e, entry 1, S1f). The diameter of AGuIX@A12, as assessed by Dynamic Light Scattering (DLS), was measured to be 6.1 nm, only slightly larger than that of AGuIX-CTGGG (4.1 nm) (Figure S1h).

The reaction was optimized to obtain a final product, AGuIX@A12, with an equimolar ratio of AGuIX NPs and A12. This was achieved by using AGuIX-Mal starting material with a high density of maleimide groups (2.1 Mal/NP). By using this starting material, a reduced amount of AGuIX NPs (and therefore Gd) could be employed to provide the same quantity of oligoglycine GGG, resulting in a lower final NP/A12 ratio from 20 to 6.0 (Figure S1e, entries 1, 2). Further reduction in the equivalence of GGG compared to A12, from 15 to 3 and 1, allowed for a decrease in the NP/A12 ratio in the final AGuIX@A12 product to 2.8 and 1.0, respectively. However, this reduction also led to a decrease in the conversion of A12, from 37% to 20% and 15%, respectively (Figure S1e, entries 2, 3, 4). To mitigate the decrease in A12 grafting during the reaction, an option was to double the amount of StrA7m while maintaining 3 equivalents of GGG compared to A12 (Figure S1e, entry 5). Interestingly, attempts to improve both A12 grafting and the final NP/A12 ratio of AGuIX@A12 by conducting sortagging at higher concentrations did not yield the desired results, likely due to the multicomponent nature of the reaction (Figure S1e, entry 6 vs 5).

In the end, sortagging proved successful in grafting VHH onto the surface of AGuIX NPs. The key parameter to increase the grafting yield of VHH was to increase the equivalence of the oligoglycine in the reaction. However, this strategy also resulted in a higher NP/A12 ratio, which ideally should be around 1 for imaging purposes. Despite increasing the GGG equivalence, achieving significantly different A12 conversion rates proved challenging, with a maximum conversion rate of less than 50%. This could be attributed to the higher rate of hydrolysis of the StrA7m-VHH complex, influenced by the increased reactivity of StrA7m.<sup>4</sup> Additionally, the residual peptide from the VHH C-terminal released during the final step of sortagging, which contains a diglycine residue at the N-terminal, may also contribute to reactivity. Ultimately, optimized conditions were able to achieve a grafting yield of 32-33% and an NP/A12 ratio of 1.2 in the final product AGuIX@A12.

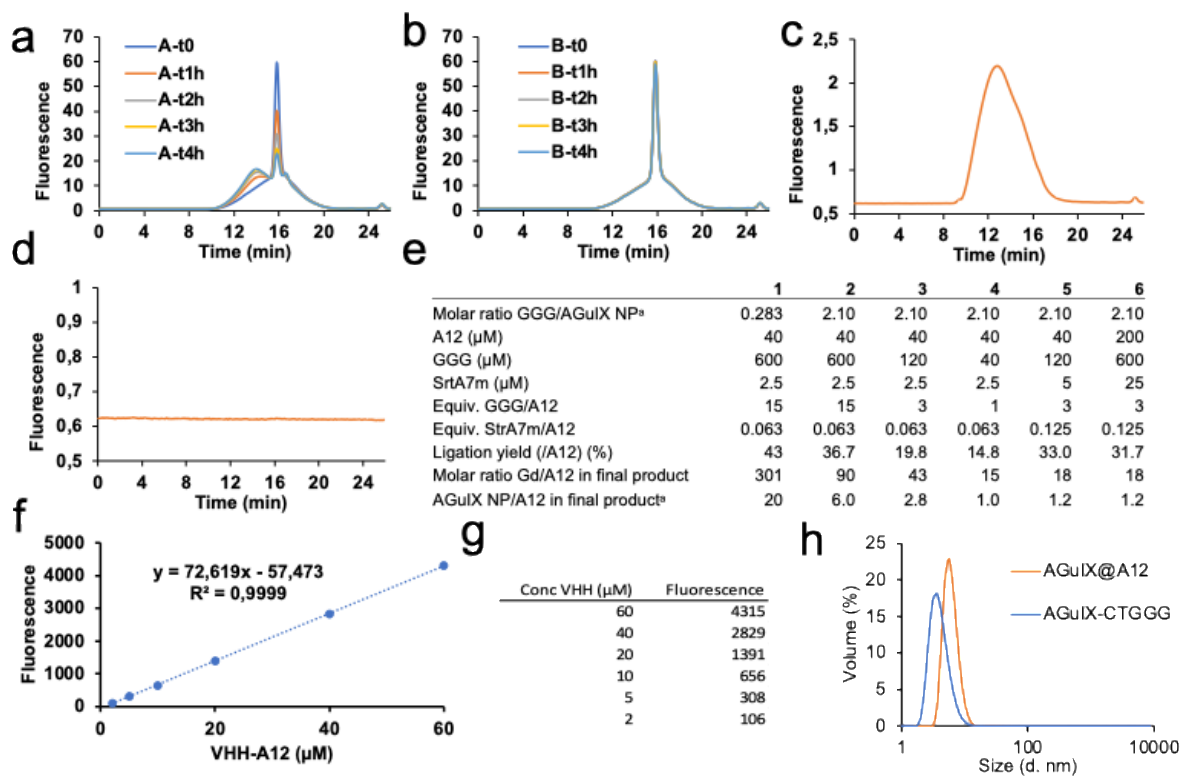


**Figure S1. Characterization on the sortagging reaction.** (a, b) Monitoring of sortagging reaction between AGuIX-CWGGG and A12 using SEC (method A, cf. main text section 2.5.1). All the reagents except StrA7m were introduced for (c), showing that no reaction happens in the absence of the enzyme. (c, d) Chromatograms of AGuIX-A12 obtained by sortagging reaction between AGuIX-CTGGG and A12 in the presence (c) and in the absence (d) of StrA7m. (e) Optimization of sortagging reaction between AGuIX-CTGGG and A12. (f) Calibration curve for A12 quantification (fluorescence, 340 nm). (g) Measurement of hydrodynamic diameter of AGuIX-CTGGG and AGuIX@A12 by DLS.

### 3. Comparison of the two chemistries

| Method                    | Sortagging reaction  | Click chemistry  |
|---------------------------|--|--|
| Number of synthesis steps | 3 steps  | 3 steps  |
| Required reagent          | GMBS<br>GGG(W/T)C peptide<br>Sortase A enzyme                                      | DBCO-PEG <sub>5</sub> -NHS<br>azide-PEG <sub>4</sub> -NHS                      |
| Reagent stability         | +  | ++<br>(DBCO-PEG <sub>5</sub> -NHS needs to be used at <20mM in aqueous medium) |
| VHH modification          | no   | yes  |
| Reaction selectivity      | High   | High   |
| Reaction speed            | Rapid (2-3h)   | Moderate (24h)   |
| Conversion yield          | Moderate (<50%)  | High (>95%)  |
| Final purification        | Sortase elimination + SEC preparative<br>(no elimination of excess AGuIX possible) | SEC preparative<br>(all excess reagents can be removed)                        |
| Ratio NP/VHH              | 1  | 1  |
| DH (nm)                   | 6.1 ± 3.7 nm   | 5.4 ± 3.1 nm   |
| Reaction costs            | High<br>(Biomolecule production)   | Moderate   |
| Scale-up potential        | Low  | High   |

**Table S1.** Summary of the comparison between the two methods, "sortagging reaction" and "click chemistry," for grafting AGuIX with a VHH

### 4. ELISA experiments

**The** One site – Fit  $K_i$  and calculated with the following formula:

Top and Bottom are the plateaus in the units of the y-axis.  $\log_{K_i}$  is the log of the molar equilibrium dissociation constant of the unlabeled ligand (AGuIX, AGuIX@A12, or AGuIX@A4). RadioligandNM is the concentration of the labeled ligand (biotin-anti-PD-L1 or biotin-anti-CD47) and HotKdNM is the equilibrium dissociation constant of the labeled ligand (biotin-anti-PD-L1 or biotin-anti-CD47).

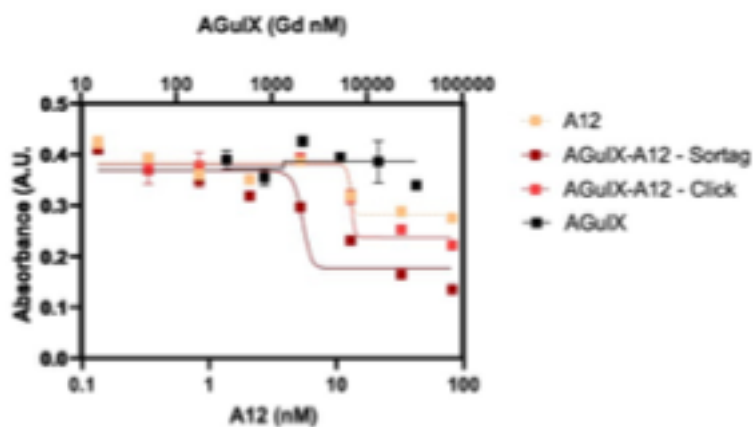


**Figure S2.** Binding affinity of AGuIX@A12 conjugates obtained from sortagging and click chemistry. ELISA plates were coated with PD-L1 proteins and affinity of free A12, AGuIX and AGuIX@A12 were assessed. No difference in binding affinity for A12 free VHH compared to AGuIX bound regardless of chemistry (Click or Sortagging) validating that functional

targeting capabilities of A12 are not impacted by the conjugation method. Control of AGuIX further confirm that binding is due to presence of A12 rather than non-specific NP and protein interactions (n=3).

## 5. Synthesis of click chemistry reaction.

### 5.1. Grafting azido-PEG<sub>4</sub>-NHS ester on VHH

A12 VHH (1.3  $\mu\text{mol}$ , 1  $\text{mg}\cdot\text{mL}^{-1}$  final concentration in reaction) were mixed with azido-PEG<sub>5</sub>-NHS (0.14  $\mu\text{mol}$ , 7  $\mu\text{M}$  final concentration in reaction) at 4 °C for 2 h. There was no post-reaction purification step to minimize VHH losses on the purification membranes. Azide grafting was characterized by SEC and MALDI-TOF (Fig. S3.a and b).

### 5.2. Grafting DBCO-PEG<sub>5</sub>-NHS ester on NPs

#### *Step 1 – Introduction of Cy5.5*

AGuIX NP (1 g, 13.51 w%Gd, 50 mg AGuIX/mL final concentration in reaction, redispersed in MilliQ H<sub>2</sub>O) and Cy5.5-NHS ester (1.72  $\mu\text{mol}$ , 85.9  $\mu\text{M}$  final concentration in reaction) were introduced in H<sub>2</sub>O (final volume 20 mL). The mixture was stirred at RT for 30 min. After x2 dilution in H<sub>2</sub>O, the AGuIX-Cy5.5 was purified by filtration (5 kDa MWCO vivaspin, dilution x2).

#### *Step 2 – Introduction of DBCO*

AGuIX-Cy5.5 NPs (774  $\mu\text{mol}$  Gd, 50 mg AGuIX/mL final concentration in reaction) were dispersed in Milli-Q water. Dibenzylcyclooctyne-PEG<sub>5</sub>-NHS (DBCO) was dissolved in dry DMSO (155  $\mu\text{mol}$ , 20 mM final concentration in reaction), added to the AGuIX-Cy5.5 solution (final volume 18 mL) and the mixture was stirred for another 2 h. The final product AGuIX-Cy5.5-DBCO was finally filtered (5 kDa MWCO vivaspin, dilution x5000) until no more DBCO moiety could be detected in the filtrate and was finally dispersed into 9 mL of MilliQ water before lyophilisation. DBCO quantification was performed by incubation with the fluorescent dye AF647@azide (24 h, RT). The determination of reacted DBCO was done by using AF647 calibration curve with the SEC method B. (Fig. S3.d) (cf. method B, fluorescence detection ex/em: 650/665 nm).

### 5.3. Optimization of the click chemistry reaction

The first step of the synthesis involves functionalizing the VHH with the azide group. A12, which contains 9 lysine residues, was used for this purpose. These residues were able to react with the azide-PEG<sub>4</sub>-NHS ester to introduce the azide group onto the VHH surface.<sup>5-7</sup> Although VHH has a chemically and physically robust structure, a ratio higher than an equimolar ratio of NHS per amine function led to its precipitation. The instability can be attributed to the alteration in charge of amino acids following the reaction, resulting in reduced solubility of the VHH.<sup>8</sup> A ratio slightly below equimolar solved this issue and we were able to successfully obtain the A12-azide. Functionalization was confirmed by Size Exclusion Chromatography (SEC) with a lower retention time suggesting an increase in size (Fig S3a). These findings were validated using Matrix-assisted laser desorption/ionization-time of flight (MALDI-TOF) mass spectrometry, a highly sensitive technique that enables reliable determination of biomolecule size.<sup>9</sup> This analytical method enabled precise evaluation of azide linker grafting, revealing a distribution of 1 to 3 linkers per A12 VHH. Additionally, it confirmed the complete grafting of all VHH in solution, as evidenced by the almost complete conversion of the initial A12 peak (14.78 kDa) (Fig S3.b.).

A second surface modification was necessary to enable the reactivity of AGuIX NPs with A12. Within the polysiloxane structure AGuIX contain primary amines in the 3-Aminopropyl)triethoxysilane (APTES) function.<sup>10,11</sup> Each NP was estimated to possess a similar number of amine functions as gadolinium chelate or gadolinium, averaging 15 gadolinium (Gd) atoms per particle.<sup>12</sup> This provided approximately the same number of amine sites on the NP surface that can be accessed for modification.<sup>13,14</sup> The AGuIX-DBCO was prepared by reacting the NHS group on the DBCO-PEG<sub>4</sub>-NHS with the primary amines on the nanoparticle surface. The objective was to achieve at least one functional group per nanoparticle. There were two limiting factors to consider for this reaction: 1) the concentration of DBCO in the solution should not exceed 20 mM to prevent linker precipitation and 2) the percentage of dimethyl sulfoxide (DMSO) in the aqueous solution should not exceed 60% to avoid the precipitation of AGuIX NPs. These factors needed to be carefully controlled to ensure successful synthesis of AGuIX-DBCO. Thus, ratios ranging from 0.15 to 5 DBCO per particle was tested to optimize the synthesis of AGuIX-DBCO (Fig S3.c.). Considering the limiting factors, the maximum achievable ratio for the synthesis of AGuIX NPs was 5 DBCO molecules per particle. Based on the calibration curve analysis, the resulting product exhibited a ratio of 10 Gd/DBCO (Fig S3.d). Given that there are 15 Gd per particle, this outcome indicated an average of at least one or two DBCO molecules per particle. This confirmed that the minimum target of one functional group per nanoparticle has been successfully achieved.

The click reaction between the azide and DBCO moieties was primarily monitored through size-exclusion chromatography (SEC)(Fig. S2e and S2f). Due to the distinct separation of the three products (AGuIX-DBCO, A12-azide and AGuIX@A12) equally facilitated the selection of SEC as the preferred purification method. The purified product underwent concentration and analysis using SEC-HPLC and SEC-HPLC-ICPMS to compare the elution profiles of gadolinium (to verify the presence of AGuIX), fluorescence (indicative of A12), and absorbance (related to the two products). The precise alignment of these three

chromatograms and the absence of compounds with retention times exceeding 15 minutes confirmed the successful attainment of a pure bioconjugate (Fig. S3g).

To characterize AGuIX@A12 and to determine the number of NPs attached per VHH, ICPMS analysis was conducted to measure the gadolinium concentration, which directly correlates with the nanoparticle concentration. The gadolinium concentration in AGuIX was determined to be  $0.02 \text{ g L}^{-1}$  or  $1.5 \text{ g L}^{-1}$ . Fluorescence analysis was employed to quantify the VHH concentration. The fluorescence signals of the AGuIX@A12 are originated from two sources: 1) the VHH component of A12 and 2) the click linkers (azide-DBCO). For better accuracy, a calibration curve was established using the fluorescence of A12@azide-DBCO in the presence of AGuIX (non-grafted) at a concentration of  $1.5 \text{ g L}^{-1}$  (Fig S2.h). The concentration of A12 was determined to be  $63 \text{ }\mu\text{M}$  in the presence of  $1278 \text{ }\mu\text{M Gd}$  (ICP/MS), corresponding to a ratio of approximately 20 Gd per VHH.

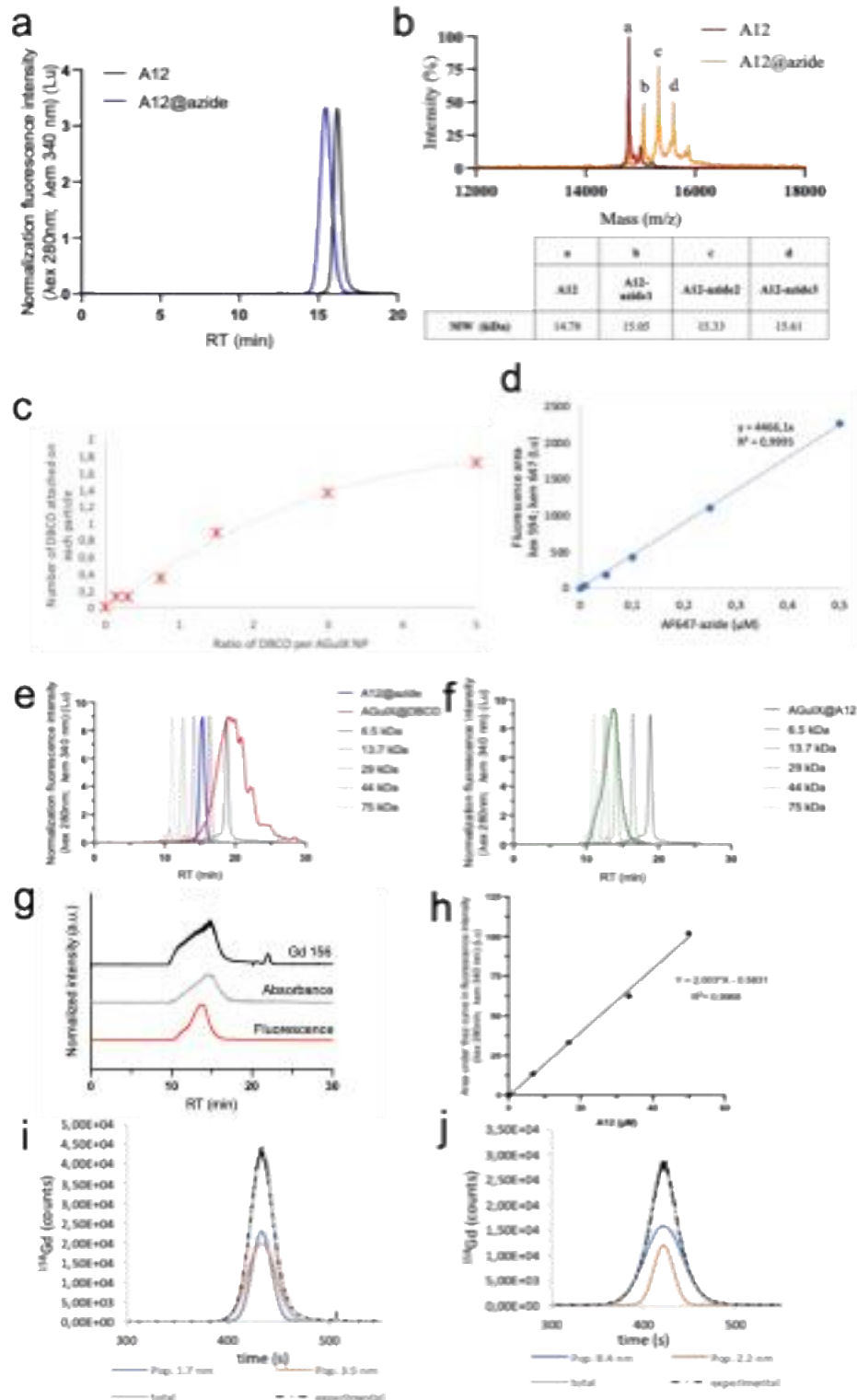


**Figure S3. Characterization on the click chemistry.** The first step of the synthesis involves functionalizing the A12 VHH with the azide group. (a) Functionalization was confirmed by Size Exclusion Chromatography (SEC) with a lower retention time suggesting an increase in size. (b) This result was validated by Matrix-assisted laser desorption/ionization-time of flight (MALDI-TOF) mass spectrometry, revealing a distribution of 1 to 3 linkers per A12 VHH. The second step of the synthesis involves functionalizing the AGuIX with the DBCO group. (c) Optimization of the DBCO/AGuIX ratio of the protocol to obtain more than one function per NP. (d) Fluorescence area calibration curve of AF647-azide dye at 647nm depending on the dye concentration to quantify the DBCO grafted on AGuIX. The area was measured by SEC (Superdex 75 column). Following of the click reaction: (e) The clear separation of the two initial products A12@azide (blue) and AGuIX@DBCO (red), enables click

bioconjugation to be followed up, and (f) formation of the AGuIX@A12 product. (g) SEC chromatogram of the purified bioconjugate following the gadolinium 156 by HPLC-ICPMS, the fluorescence ( $\lambda_{exc}=280$  nm;  $\lambda_{em}=340$  nm) and absorbance ( $\lambda=295$  nm) by HPLC UV-vis. (h) Calibration curve of fluorescence area ( $\lambda_{exc}=280$  nm;  $\lambda_{em}=340$  nm) versus A12@azide-DBCO concentration was done to quantify the VHH in the final product. Analysis performed on Agilent HPLC on Superdex 75 10/300 column and data processed on GraphPad 8.0.1 Representative taylorgram and corresponding bimodal fit for gadolinium signal for (i) AGuIX-DBCO nanoparticles and (j) AGuIX@A12 after purification. The signal (dashed black line) was fitted with the sum (solid gray line) of two gaussian curves (solid blue and orange lines) of the two populations within the sample.

## 6. Material characterizations

### 6.1. Taylor Dispersion Analysis (TDA)

TDA experiments were conducted using a TDA –ICP-MS hyphenation between a Sciex P/ACE MDQ instrument and a 7700 Agilent ICP-MS, described elsewhere.<sup>15</sup> Fused silica capillaries with an inner diameter of 75  $\mu$ m and outer diameter of 375  $\mu$ m, and a total length of 64 cm, were coated with hydroxypropylcellulose (HPC) using a solution of 0.05 g/mL in water. The capillaries were then subjected to injection (5 psi for 3 s, equivalent to 15 nL), and the samples were mobilized by applying a pressure of 0.7 psi using a Tris 10 mM, NaCl 15 mM buffer at pH 7.4. Detection was carried out by ICP-MS at  $m/z=158$  with a data acquisition rate of 500 ms/point. Between runs, the capillary was flushed at 10 psi for 5 min with the mobilization medium.

The taylorgrams obtained by TDA can be assimilated to the sum of several Gaussians signals:

(1)

where  $t_{0i}$  is the peak residence time and  $A_i$  and  $\sigma_i$  are the area under the curve and temporal variance associated to the different species  $i$ , respectively. Equation 2 relates the molecular diffusion coefficient  $D$  to the hydrodynamic radius of the species under the specified experimental conditions.

(2)

where  $r_c$  is the capillary radius,  $k_B$  is the Boltzmann constant,  $T$  is the temperature,  $\eta$  is the viscosity, and  $R_h$  is the hydrodynamic radius of the species. The viscosity of a Tris 10 mM, NaCl 15 mM buffer was previously determined to be 0.908. Peak deconvolution was carried out using Origin 8.5 software.

### 6.2. Matrix-Assisted Laser Desorption Ionization – Time of Flight mass spectrometry (MALDI-TOF MS)

The mass spectrum was generated using a Voyager-DE PRO (Sciex, Framingham, Massachusetts) equipped with a nitrogen laser that emitted at 337 nm with a 2 ns pulse. To create the mass spectrum, the ions were accelerated to a final potential of 25 kV, and 300 laser shots were summed together. An external mass calibration was performed using a mixture of proteins from the Sequazyme™ standards kit (Sciex). The analysis was conducted in linear mode with an instrument mass accuracy of 0.05%. To prepare the samples, the protein solution (1 g L<sup>-1</sup>) was diluted 20-fold in a matrix of sinapinic acid (SA, Sigma-Aldrich) and dissolved in 0.1%TFA/acetonitrile (70/30, v/v). Finally, 1  $\mu$ L of the mixture was utilized for analysis.

### 6.3. Biacore analyses

#### 6.3.1. Materiel method

Biomolecular interactions between immobilized receptor PD-L1 and CD47 and analyte AGuIX@A12 or AGuIX@A4 were assessed by Surface Plasmon Resonance (SPR) on Biacore 2000 instrument (Cytiva). The instrument was equipped with a CM5 sensor chip carrying a carboxymethylated dextran matrix covalently attached to a gold surface (Cytiva). The chip is connected to a microfluidic system that allows the flow of samples on the chip surface. All SPR experiments were performed at RT in HEPES (HBS-P, GE Healthcare, 0.01 M HEPES, 0.15 M NaCl, 0.005% surfactant P20) as running buffer. The four channels of the chip (fc1, fc2, fc3 and fc4) were used for this study and two were used as reference (fc1 and fc3). First, each channel was activated with a mixture of 1-ethyl-3-(3-dimethylaminopropyl) carbodiimide (EDC)/N-hydroxysuccinimide (NHS) (0.2 M EDC/0.05 M NHS) during 7 min to generate reactive succinimide esters. Following, PD-L1 and CD47 receptors were injected on the fc2 and fc4 channel, respectively, at 10  $\mu$ g/ml in acetate buffer pH 4.5 for the PD-L1 and pH 5 for the CD47 at a flow rate of 5  $\mu$ L min<sup>-1</sup> for 24 min (PD-L1) and 12min (CD47). Covalent immobilization of the receptors (PD-L1 and CD47) on the surface of the sensor chip was confirmed by an increase of 1040 response units (RU) for fc2 and 1600 RU for fc4. The unreacted succinimide esters were deactivated by ethanolamine (pH 8.5) during 7 min at a flow rate of 5  $\mu$ L min<sup>-1</sup>. The fc1 and fc3 were used as a control for nonspecific interaction and the succinimide esters were directly deactivated with ethanolamine without adding receptors. For the analysis of the different samples, they were injected on all channel by several cycles. A cycle corresponds to an injection of the sample for 3 min at a flow rate of 30  $\mu$ L min<sup>-1</sup> followed by a stabilization period of 2.5 min under the running buffer (HBS-P) then followed by a regeneration solution (1 M NaCl and 5 mM NaOH) for 30-60 s at a flow rate of 30  $\mu$ L min<sup>-1</sup> and finally another stabilization period of 2 min. For the kinetic assays, the A12 was injected at the 0 - 61.2 nM concentration range, the A4 at 0-67 nM, the AGuIX NPs at 0-915.7 nM in Gd<sup>3+</sup>, the AGuIX@A12 VHH at 0-61.2 nM, (0-915.7 nM equivalent in Gd<sup>3+</sup>) and the AGuIX@A4 VHH at 0-16.65 nM (0-250 nM equivalent in Gd<sup>3+</sup>). Each experiment began with three cycles of operating buffer injection to stabilize the baseline of the instrument. Then, the concentration gradients of the samples (AGuIX, VHHs and bioconjugates) were analyzed 3 times. All characteristic interaction constants (equilibrium

dissociation ( $K_D$ ), kinetic rate of association and dissociation ( $k_A$  and  $k_D$ ) were determined by curve fitting using the Langmuir 1:1 binding model implemented in Biaevaluation software 4.1.1.<sup>16</sup> Prior to the calculations, the signals were plotted on a sensogram by subtracting the nonspecific signal from the control channels (fc1 and fc3), from the signal obtained from the functionalized channels (respectively fc2 and fc4). Concerning the characteristic constants, the number of complexes analyte-receptor formed per second in a molar solution of VHH and receptor is described by the association rate constant  $k_a$  (in  $M^{-1} s^{-1}$ ) defined by the formula : with A the analyte (VHH or NPs) and B the ligand (receptor) and AB the final complex analyte-ligand. The number of complexes dissociated per second; they are determined by the dissociation rate constant  $k_d$  (in  $s^{-1}$ ) given by the formula:  $\frac{d[AB]}{dt} = k_a[A][B]$ . The association and the dissociation are two phenomena that happen at the same time, and at equilibrium they are equal. This equilibrium is defined by an equilibrium dissociation constant  $K_D$  obtained by the formula:  $K_D = \frac{[A][B]}{[AB]} = \frac{k_a}{k_d}$ . According to the  $K_D$  formula, the lower its the value, the stronger the interaction between the analyte and the receptor. The Langmuir 1:1 binding model implemented in Biaevaluation 4.1.1.1 software was used to analyze the sensograms and to determine the interaction constants ( $K_D$ ,  $k_A$  and  $k_D$ ) associated to each sample.

### 6.3.2. Results

The association rate constants were assessed for the PD-L1 receptor, revealing that A12 exhibits remarkably high affinity, approximately 10 times greater than that of A4 (specifically,  $k_a$ , A12 =  $(21.10 \pm 2.21) \times 10^5$  and  $k_a$ , A4 =  $(1.15 \pm 0.10) \times 10^5$ ) (Fig. S4.b&d). Conversely, the dissociation rate constant was four times faster for A4 than for A12 (namely,  $k_d$ , A4 =  $(42.10 \pm 1.64) \times 10^{-4}$  and  $k_d$ , A12 =  $(13.20 \pm 1.10) \times 10^{-4} s^{-1}$ ) (Fig. S4.b&d). These results confirmed that A12 possessed significantly higher affinity for PD-L1 compared to the nanobody A4, emphasizing the specificity of the interaction between the nanobody and the receptor. The same trends were observed for the bioconjugates, where AGuIX@A12 exhibited approximately 10 times higher affinity than AGuIX@A4 for the PD-L1 receptor ( $k_a$ , AGuIX@A12 =  $(15.50 \pm 2.55) \times 10^5$  and  $k_a$ , AGuIX@A4 =  $(1.37 \pm 0.05) \times 10^5 M^{-1} \cdot s^{-1}$ ) (Fig. S4.c&e). Dissociation rates were also faster for AGuIX@A4, consistent with the reference nanobodies ( $k_d$ , AGuIX@A12 =  $6.0 \times 10^{-4}$  and  $k_d$ , AGuIX@A4 =  $11.8 \times 10^{-4} s^{-1}$ ) (Fig. S4.c&e). These findings highlighted A12's strong specificity for the PD-L1 receptor, whether grafted onto AGuIX or not.

For the CD47 receptor, specificity was observed only with A4. Neither A12 nor AGuIX alone showed any affinity for CD47. Similar orders of magnitude for association and dissociation rates were obtained between the conjugate and the reference VHH ( $k_a$ , A4 =  $11.4 \times 10^5$  and  $k_a$ , AGuIX@A4 =  $6.7 \times 10^5 M^{-1} s^{-1}$ , and  $k_d$ , A4 =  $7.9 \times 10^{-4}$  and  $k_d$ , AGuIX@A4 =  $4.9 \times 10^{-4} s^{-1}$ ) (Fig. S5)., confirming once again the preservation of VHH functionality even after functionalization with AGuIX.

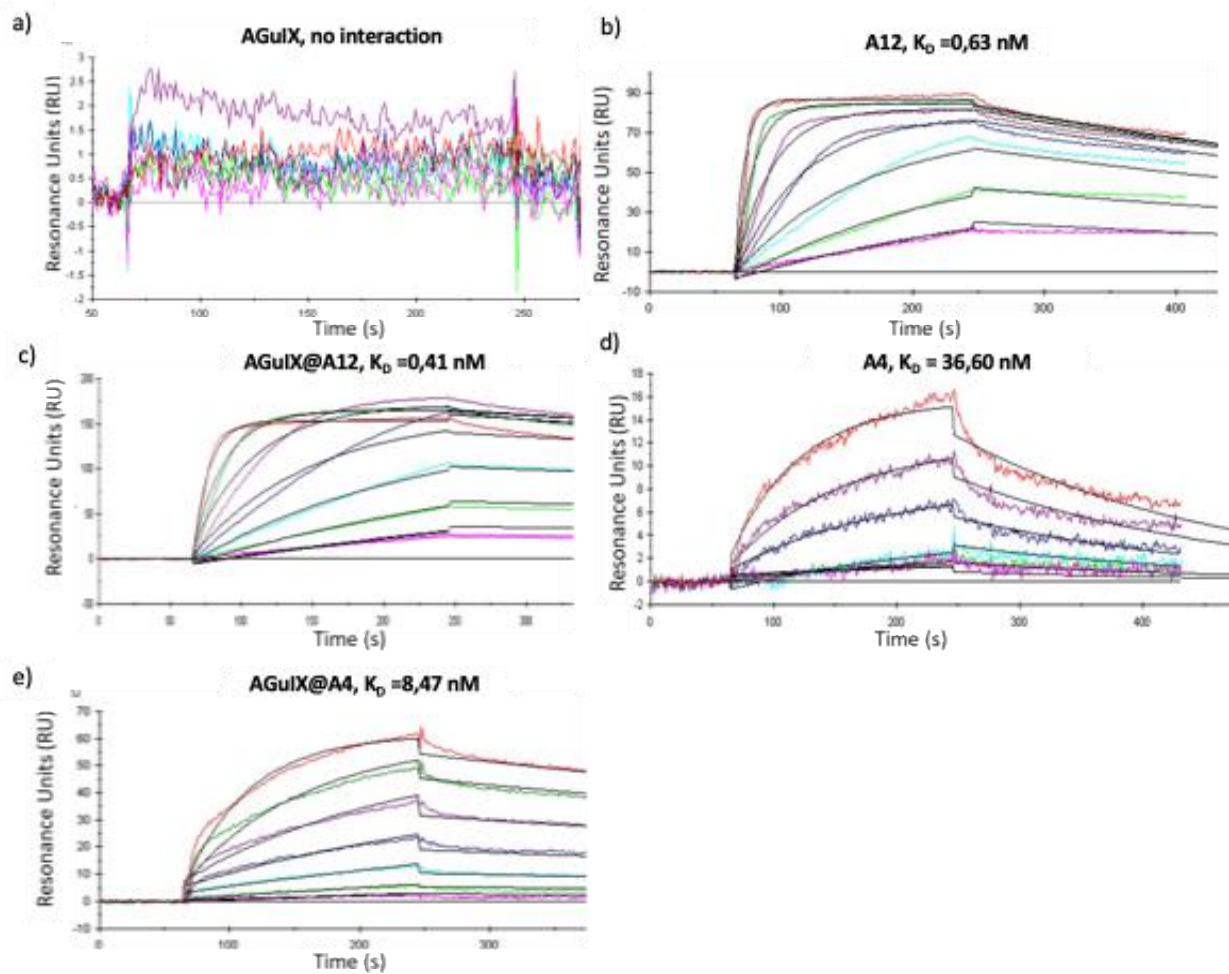


**Figure S4. Affinity measurement on PD-L1 using Biacore®.** Curve fitting (in black) of the experimental data (in color) corresponding to phase of association and dissociation of samples at various concentration on the PD-L1 receptor immobilized on the surface of the sensor chip in the channel fc2. The signal corresponds to the fc2-fc1 channel as a function of time. Sensorgram of SPR responses of compound AGuIX (0 to 915.7 nM in Gd<sup>3+</sup>) (a), A12 (0 to 61.2 nM in VHH) (b), AGuIX@A12 (0 to 61.2 nM in VHH) (c), A4 (0 to 67nM in VHH) (d) and AGuIX@A4 (0 to 67nM in VHH) (e) with PD-L1. Triplicates were made for all measurements.

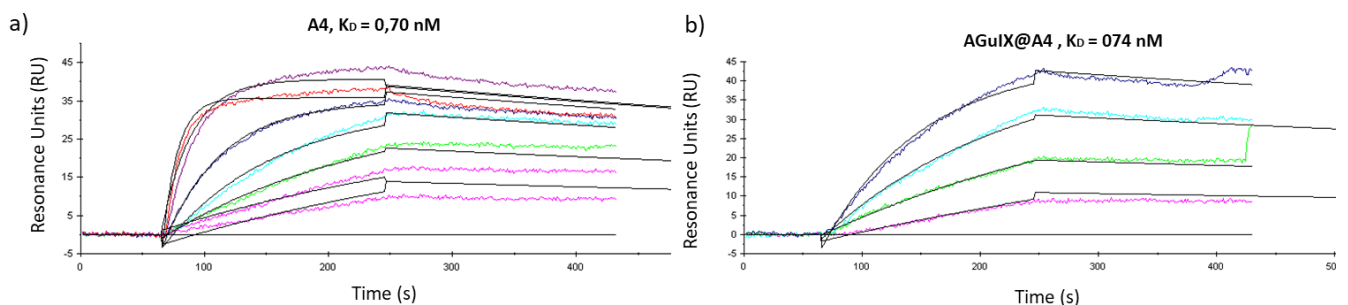


**Figure S5. Affinity measurement on CD47 using Biacore®.** Curve fitting (in black) of the experimental data (in color) corresponding to phase of association and dissociation of samples at various concentration on the CD47 receptor immobilized on the surface of the sensor chip in the channel fc4. The signal corresponds to the fc4-fc3 channel as a function of time. Sensorgram of SPR responses of compound A4 (0 to 67nM in VHH) (a) and AGuIX@A4 (0 to 0-16.65nM in VHH) (b) with CD47.

Triplicates was made for A4. Due to a chip regeneration problem and the lack of product, only one analysis was carried out on A4@AGuIX.

#### 7. <sup>89</sup>Zr-Radiolabeling of AGuIX and AGuIX-A12

AGuIX-A12 have been radiolabeled with zirconium-89 (<sup>89</sup>Zr) according to the protocol described by Tran *et al.*<sup>17</sup> Briefly, 40 μg of AGuIX and 40 μg of AGuIX-A12, pH adjusted to 7.2, were incubated in a solution containing neutralized [<sup>89</sup>Zr][Zr-(oxalate)<sub>4</sub>]<sup>4-</sup> for 15 min at 37 °C, 300 rpm. The oxalic acid of the <sup>89</sup>Zr oxalate solution from Perkin Elmer (200 μL, 430 MBq) was neutralized with 90 μL of Na<sub>2</sub>CO<sub>3</sub> (2 M) before adding them to the AGuIX-based solutions. The radiochemical purity of [<sup>89</sup>Zr]-AGuIX and [<sup>89</sup>Zr]-AGuIX-A12 was assessed by Thin Layer Chromatography (TLC). 5 μL of samples from the reaction were taken after 15 min incubation to deposit on a chromatography paper (1 × 12 cm). These TLC papers were migrated in citrate sodium buffer, pH 5.5, and the activity was measured using a Mini-Scan TLC Imaging Scanner with gamma detector B-FC-3600 (Eckert & Ziegler, Germany) at 1.0 mm.s<sup>-1</sup>. High radiolabeling yield was obtained reaching 99% and 94% for [<sup>89</sup>Zr]-AGuIX and [<sup>89</sup>Zr]-AGuIX-A12 respectively. [<sup>89</sup>Zr]-AGuIX and [<sup>89</sup>Zr]-AGuIX-A12 were purified and concentrated by Vivaspin® ultrafiltration tubes (Sartorius, 5 kDa MWCO). Specific activities were 0.29 and 0.32 MBq/μg AGuIX for [<sup>89</sup>Zr]-AGuIX and [<sup>89</sup>Zr]-AGuIX-A12 respectively.

| <sup>89</sup> Zr labeled AGuIX | Specific activity (μCi/μg Gd) | Injected activity (μCi) | Number of mice/Time point | Radiolabeling Yield by iTLC |
|--------------------------------|-------------------------------|-------------------------|---------------------------|-----------------------------|
| AGuIX-A12                      | 7.3                           | 52 +/- 3                | 4                         | 94%                         |
| AGuIX                          | 8.6                           | 62 +/- 2                | 4                         | 99%                         |

Table S2. <sup>89</sup>Zr-Radiolabeling of AGuIX and AGuIX-A12.

#### 8. Proof of concept on A4 VHH

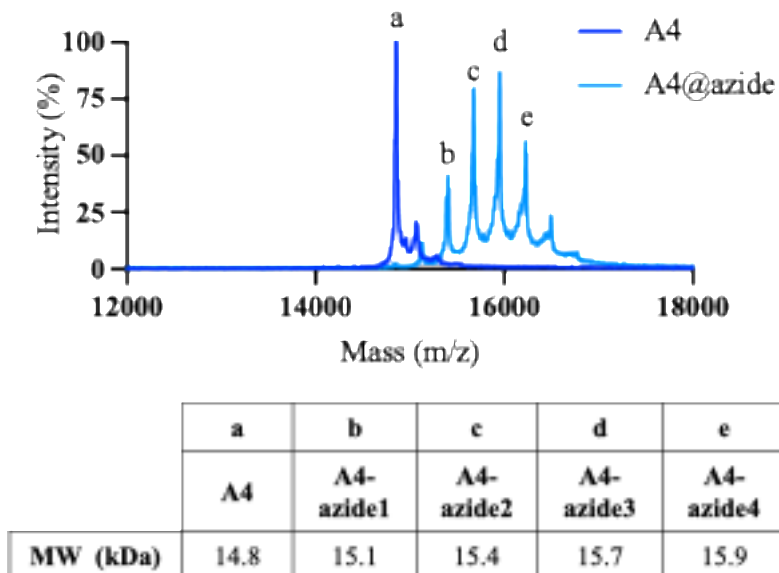
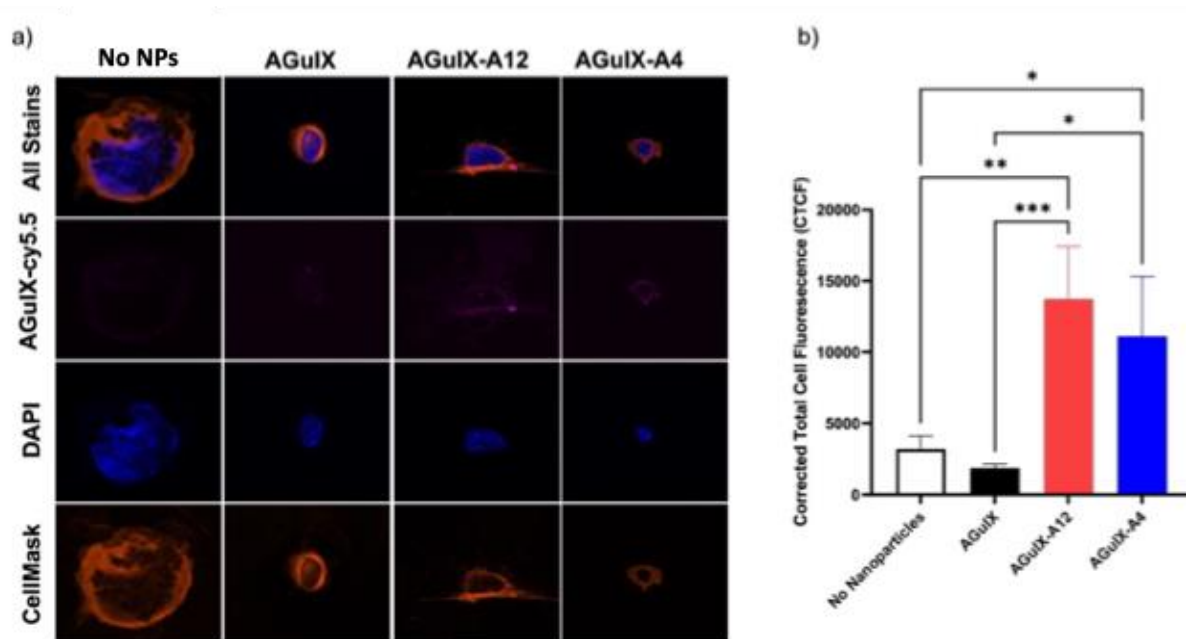


Figure S6. A4 modification with the linker azide-PEG<sub>4</sub>-NHS confirmed by MALDI-TOF analysis. The results revealed a distribution of 1 to 4 linkers per A4 VHH. It confirmed the complete grafting of all VHH in solution, as evidenced by the almost complete conversion of the initial A4 peak (14.85 kDa).



**Figure S7.** Internalization of AGuIX-VHH in wild-type melanoma. (a) Metastatic wild-type B16F10 cells were incubated with either Cy5.5 conjugated AGuIX or AGuIX-VHH (magenta) for 1 h prior to staining with CellMask plasma membrane (orange) and DAPI (blue) nuclear stain. (b) AGuIX and AGuIX-VHH fluorescence was quantified using ImageJ software to calculate corrected total cell fluorescence, CTCF ( $n = 5 - 10$  cells, \*  $p < 0.05$ , \*\*  $p < 0.01$ , \*\*\*  $p < 0.001$ ).

## References

- 1 J. R. Ingram, M. Dougan, M. Rashidian, M. Knoll, E. J. Keliher, S. Garrett, S. Garforth, O. S. Blomberg, C. Espinosa, A. Bhan, S. C. Almo, R. Weissleder, H. Lodish, S. K. Dougan and H. L. Ploegh, *Nat. Commun.*, 2017, **8**, 647.
- 2 M. Dougan, J. R. Ingram, H.-J. Jeong, M. M. Mosaheb, P. T. Bruck, L. Ali, N. Pishesha, O. Blomberg, P. M. Tyler, M. M. Servos, M. Rashidian, Q.-D. Nguyen, U. H. von Andrian, H. L. Ploegh and S. K. Dougan, *Cancer Immunol. Res.*, 2018, **6**, 389–401.
- 3 J. T. Sockolosky, M. Dougan, J. R. Ingram, C. C. M. Ho, M. J. Kauke, S. C. Almo, H. L. Ploegh and K. C. Garcia, *Proc. Natl. Acad. Sci. U. S. A.*, 2016, **113**, E2646–E2654.
- 4 H. E. Morgan, W. B. Turnbull and M. E. Webb, *Chem. Soc. Rev.*, 2022, **51**, 4121–4145.
- 5 N. Asiiimwe, M. F. Al Mazid, D. P. Murale, Y. K. Kim and J.-S. Lee, *Pept. Sci.*, 2022, **114**, e24235.
- 6 S. Mädler, C. Bich, D. Touboul and R. Zenobi, *J. Mass Spectrom.*, 2009, **44**, 694–706.
- 7 J. S. Nanda and J. R. Lorsch, in *Methods in Enzymology*, ed. J. Lorsch, Academic Press, 2014, vol. 536, pp. 87–94.
- 8 C. J. Pickens, S. N. Johnson, M. M. Pressnall, M. A. Leon and C. J. Berkland, *Bioconjug. Chem.*, 2018, **29**, 686–701.
- 9 V. Solntceva, M. Kostrzewa and G. Larrouy-Maumus, *Front. Cell. Infect. Microbiol.*, 2021, **10**, 621452.
- 10 C. Truillet, E. Thomas, F. Lux, L. T. Huynh, O. Tillement and M. J. Evans, *Mol. Pharm.*, 2016, **13**, 2596–2601.
- 11 E. Thomas, L. Colombeau, M. Gries, T. Peterlini, C. Mathieu, N. Thomas, C. Boura, C. Frochot, R. Vanderesse, F. Lux, M. Barberi-Heyob and O. Tillement, *Int. J. Nanomedicine*, 2017, **Volume 12**, 7075–7088.
- 12 N. Brown, P. Rocchi, L. Carmès, R. Guthier, M. Iyer, L. Seban, T. Morris, S. Bennett, M. Lavelle, J. Penailillo, R. Carrasco, C. Williams, E. Huynh, Z. Han, E. Kaza, T. Doussineau, S. M. Toprani, X. Qin, Z. D. Nagel, K. A. Sarosiek, A. Hagège, S. Dufort, G. Bort, F. Lux, O. Tillement and R. Berbeco, *Theranostics*, 2023, **13**, 4711–4729.
- 13 E. Thomas, C. Mathieu, P. Moreno-Gaona, V. Mittelheisser, F. Lux, O. Tillement, X. Pivot, P. P. Ghoroghchian and A. Detappe, *Adv. Healthc. Mater.*, 2022, **11**, 2101565.
- 14 E. Thomas, Cancer, Université de Lyon, 2017.
- 15 L. Labied, P. Rocchi, T. Doussineau, J. Randon, O. Tillement, F. Lux and A. Hagège, *Anal. Chem.*, 2021, **93**, 1254–1259.
- 16 L. Heinrich, N. Tissot, D. J. Hartmann and R. Cohen, *J. Immunol. Methods*, 2010, **352**, 13–22.
- 17 V.-L. Tran, F. Lux, N. Tournier, B. Jego, X. Maître, M. Anisorac, C. Comtat, S. Jan, K. Selmecci, M. J. Evans, O. Tillement, B. Kuhnast and C. Truillet, *Adv. Healthc. Mater.*, 2021, **10**, e2100656.